Time-optimal chaos control by center manifold targeting

John Starrett
Department of Mathematics, University of Colorado, 3500 Clay Street, Denver, Colorado 80211
(Received 22 May 2002; published 10 October 2002)

Ott-Grebogi-Yorke control and its map-based variants work by targeting the (linear) stable subspace of the target orbit so that after one application of the control the system will be in this subspace. I propose an *n*-step variation, where *n* is the dimension of the system, that sends any initial condition in a controllable region directly to the target orbit instead of its stable subspace. This method is time optimal, in that, up to modeling and measurement error, the system is completely controlled after *n* iterations of the control procedure. I demonstrate the procedure using a piecewise linear and a nonlinear two-dimensional map, and indicate how the technique may be extended to maps and flows of higher dimension.

DOI: 10.1103/PhysRevE.66.046206 PACS number(s): 05.45.Gg

I. INTRODUCTION

Since the paper of Ott, Grebogi, and Yorke (OGY) [1] on controlling chaotic dynamical systems appeared in 1990, there have been many methods designed explicitly to control chaotic dynamics by stabilizing the saddle orbits already present in an attractor. Questions immediately arose about the relation of OGY control to the traditional control theory, including the question of optimality. Romeiras *et al.* [2] pointed out that OGY control was equivalent to making a particular choice of regulator poles, and thus was a specialized implementation of the pole placement problem of the classical control theory. Chen [3] has suggested an energy-optimal approach using the classical theory of optimal control to control the saddle orbits in an attractor.

II. OGY AND CLASSICAL LINEAR CONTROL THEORY

To implement OGY control, we locate a target orbit $\overline{\mathbf{x}}$ in the attractor and assume the local dynamics are well modeled by a linear map $\mathbf{x}_{i+1}-\overline{\mathbf{x}}=A(\mathbf{x}_i-\overline{\mathbf{x}})+\mathbf{g}(\rho_i-\rho_0)$ where A is an $n\times n$ matrix, $\mathbf{g}=\partial\overline{\mathbf{x}}/\partial\rho$ and ρ_0 is the nominal value of the scalar control parameter ρ_i. The aim is to choose ρ_i so that the system state is steered to the stable manifold, represented in the linear approximation by the stable eigenvector $\mathbf{e}_s$, after a time T, the period of the target orbit $\overline{\mathbf{x}}$. To approach the problem as one of the classical linear control by the pole placement, we assume $\delta\rho_i=\rho_i-\rho_0$ is of the form $\delta\rho_i=-\mathbf{c}^T(\mathbf{x}_i-\overline{\mathbf{x}})$ where $\mathbf{c}$ is a constant vector. Setting $\delta\mathbf{x}_i=\mathbf{x}_i-\overline{\mathbf{x}}$, we obtain $\delta\mathbf{x}_{i+1}=(A-\mathbf{g}\mathbf{c}^T)\delta\mathbf{x}_i$. If the eigenvalues of the regulator matrix $(A-\mathbf{g}\mathbf{c}^T)$ all have modulus less than one, then $\delta\mathbf{x}_i\to 0$ as $i\to\infty$. Choosing the gain vector $\mathbf{c}$ so that eigenvalues of the regulator matrix, called the *regulator poles*, are less than one in modulus is the *pole placement problem*. There are many ways to choose the regulator poles, and OGY control amounts to setting n_s of these poles to the eigenvalues of the stable eigenvectors of A and the rest to zero [2].

Optimal control

A control method is optimal when some property of a sequence of control perturbations $\rho_0,\rho_1,\ldots,\rho_{i-1}$ is minimized. An optimal control is usually either energy optimal, where the total energy $\Sigma_k\rho_k^2 w$, (w is a weighting function), is minimal, or time optimal, where the time to control is minimal. The energy-optimal solution in the context of classical linear control theory is well known [3]. I aim to address the time optimality of OGY control, and introduce a time-optimal variation on map-based OGY.

1. Time optimality of OGY

OGY control, although ''merely'' a specialization of the classical control theory is elegant because of the goal behaviors it chooses to stabilize, the infinite set of unstable periodic orbits that form the skeleton of an attractor. By its clever choice of regulator poles, OGY control is already, very loosely, time optimal in the sense that only one perturbation is required before the orbit is essentially controlled—if the system is truly linear, once the perturbation is applied, there is nothing more to be done. The system will be on the stable manifold of the target orbit and the natural dynamics of the system will thereafter, evolve the system state to the goal state. However, this is not strict time optimality, in that the system is not completely controlled, although it is approaching a controlled state exponentially.

2. Energy optimality of OGY

A chaotic system is ergodic; a chaotic orbit will eventually visit every neighborhood of the attractor, no matter how small, given enough time. OGY control can be made energy optimal by waiting long enough so that the ergodicity of the map brings the system state close enough to the stable manifold of a fixed point so that the perturbation $\delta\rho$ that places the system state on the stable manifold of the periodic orbit is as small as one desires. This is a bit of a cheat, though. A chaotic system without control is also energy optimal in the same sense, any chaotic orbit will eventually approach any target saddle orbit in the attractor as closely as we like and stay there as long as we like. What really counts is attaining the target orbit as quickly or as cheaply as possible, once we decide to control the system.

III. GLOBAL TARGETING

We seldom have the luxury of being able to wait as long as it takes just to save energy, or to expend as much energy

as it takes to save time. Shinbrot *et al.* [4] addressed the problem of steering a system state at a distant point in an attractor to the target neighborhood using the sensitivity of the system to perturbations. A controllable region around the target orbit was iterated backwards until it covered the entire attractor. Then, a sequence of small perturbations could steer any point in the attractor to the controllable region where it could be stabilized by OGY or some other local method. Bollt and Kostelich [5] used a graph theoretic approach to determine the optimum path through an attractor to the neighborhood of a target orbit, using roughly the same steering strategy. Bradley [6] proposed a method whereby a large database stored orbits for many different parameter settings, and an optimal path from the current system state to the desired system state was patched together from these orbits. The methods of Shinbrot *et al.*, Bradley, and Bollt *et al.* greatly reduce the time to navigate through an attractor to reach the neighborhood of a target orbit, but do not speak directly to the point of efficiently stabilizing that orbit once the system state attains that neighborhood.

IV. LOCAL TARGETING

There are many options besides the original method of Ott, Grebogi, and Yorke once the neighborhood of the target orbit is attained. Variations on the OGY method fall into roughly four categories:

(1) simplifications,
(2) necessary modifications,
(3) continuous time methods, and
(4) optimal methods.

Among the necessary modifications, I include those of Dressler and Nitsche [7] who modified the OGY strategy to take into account the use of time delay coordinates, and the modifications needed for controlling higher-dimensional systems [8–10] and spatiotemporal chaos [11–14]. Among the continuous time methods are those of Pyragas [15] and Socolar *et al.* [16], which control by synchronizing with a time delayed version of the current system state, and Carr and Schwartz [17] who used parameter perturbation, its duration, and the delay before application as three separate parameters to control high-dimensional continuous systems. Of these categories, the optimal methods are of the greatest relevance to the present work, while some aspects of certain simplifications are germane.

A. Simplifications

The first variations on the OGY method were simplifications that could be made if the system was well characterized by a one-dimensional map. Peng *et al.* [18] and Hunt [19] demonstrated that chemical and electronic systems, respectively, could be controlled by applying a perturbation simply proportional to the deviation of the current system state from the target orbit when the system was highly dissipative. This type of control came to be known as occasional proportional feedback (OPF), and its formulation assumed that perturbations moved the target orbit along the unstable direction. For a one-dimensional linear map whose perturbation moved the target orbit along the unstable direction, the OGY rule results in a time-optimal control for system states inside the controllable region; a single perturbation over one iterate of the map is sufficient to place the system state on the fixed point by the next iterate. Generically, however, a perturbation does not move the target orbit solely along the unstable direction, and maps are only nearly linear in a small region near the target orbit. Rollins and co-workers [20] improved on the results of Peng *et al.* and Hunt by constructing a recursive control rule (recursive proportional feedback or RPF) that corrected the OPF rule for when the perturbation moved the target orbit off the attractor.

B. Optimal methods

Reyl *et al.* [21] demonstrated the control of a nuclear magnetic resonance laser using a control rule designed so that a perturbation at step m would minimize the deviation of the system state at step $m+1$ from the target orbit. This is a kind of energy-optimal control, in that each perturbation aims, roughly, to minimize the energy needed for the next perturbation. Epureanu and Dowell [22,23] proposed a time-optimal method for continuous chaotic systems using a time-varying parameter perturbation to steer a system state directly to a target orbit, once the system state entered a controllable region. Their method requires a continuous model of the system dynamics, either in the form of an equation of motion, or a local continuous model of the dynamics between the surfaces of section, which can be built from data.

V. CONTROL BY CENTER MANIFOLD TARGETING (CMT)

While the proportional feedback methods can be close to time optimal for nearly linear, almost one-dimensional systems, they fail to be time optimal if the control perturbation moves the system state off the attractor. The method demonstrated by Epureanu and Dowell, while time optimal, requires a continuous model of the system and will not work for true maps or strict map-based models from surfaces of section.

I propose and demonstrate an n-step method, where n is the dimension of the system, that requires only knowledge of the dynamics of the surface of section map, and steers the system state directly to the target orbit, under the same linearity assumptions of OGY. There is no need for the attractor to be nearly one dimensional. The method works for maps, as well as continuous systems by targeting a sequence of lower- and lower-dimensional slabs, terminating at the zero-dimensional fixed point.

Let $\dot{\mathbf{x}}=F(\mathbf{x},t,\rho)$ be a continuous time dissipative chaotic system with one accessible scalar parameter ρ and target orbit $\underline{\mathbf{x}}(t,\rho)$ of saddle type. Designate by $\breve{\mathbf{x}}(t,\rho)$ some orbit near $\underline{\mathbf{x}}(t,\rho)$, and set $\mathbf{x}(t,\rho)=\breve{\mathbf{x}}(t,\rho)-\underline{\mathbf{x}}(t,\rho)$. If we take a surface of section transverse to $\underline{\mathbf{x}}$, then near $\underline{\mathbf{x}}$ the system can be modeled as a linear map $\mathbf{x}_{i+1}=A\mathbf{x}_i$ where A is an $n\times n$ matrix assumed to have no ρ dependency for $\delta\rho$ small. If we perturb the system by $\delta\rho$, the attractor, and hence the peri-

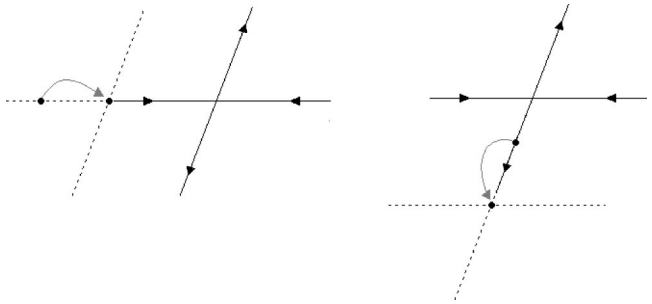

FIG. 1. This figure shows the perturbed and unperturbed manifolds during the control. The unperturbed manifolds are dashed, and the perturbed manifolds are solid. On the left, a system state on the stable manifold is brought directly to the center manifold under the perturbed dynamics. This is the special case where the perturbation moves the target orbit along the stable manifold. On the right, a system state on the unstable manifold is brought directly to the center manifold under the perturbed dynamics. This is the special case where the perturbation moved the target orbit along the unstable manifold.

odic point $\overline{\mathbf{x}}$ will shift so that $\overline{\mathbf{x}}$ moves to $\overline{\mathbf{x}}+\delta\rho\mathbf{g}$, where $\mathbf{g}=\partial\overline{\mathbf{x}}/\partial\rho$. The stable and unstable eigenvectors $\mathbf{e}_s,\mathbf{e}_u$ of A are local linear models for the stable and unstable manifolds near $\overline{\mathbf{x}}$, and to control by OGY, we perturb the system so that $\mathbf{x}$ lies in $\mathbf{e}_s$ after one iterate of the map.

Form the pair of vectors $(\mathbf{f}_u,\mathbf{f}_s)$ with the properties

$$\mathbf{f}_s\cdot\mathbf{e}_s=1,\quad \mathbf{f}_s\cdot\mathbf{e}_u=\mathbf{0},$$

$$\mathbf{f}_u\cdot\mathbf{e}_s=0,\quad \mathbf{f}_u\cdot\mathbf{e}_u=1. \tag{1}$$

The system state is in the (linear) stable subspace $\mathbf{e}_s$ when $\mathbf{x}_{i+1}\cdot\mathbf{f}_u=0$. To determine the appropriate perturbation, we solve $\mathbf{f}_u\cdot(\mathbf{x}_{i+1}-\delta\rho\mathbf{g})=\mathbf{f}_u\cdot A(\mathbf{x}_i-\delta\rho\mathbf{g})=0$ for $\delta\rho$. Since A may be decomposed as $A=[\lambda_s\mathbf{e}_s\mathbf{f}_s^T+\lambda_u\mathbf{e}_u\mathbf{f}_u^T]$, we solve

$$\mathbf{f}_u\cdot\{[\lambda_s\mathbf{e}_s\mathbf{f}_s^T+\lambda_u\mathbf{e}_u\mathbf{f}_u^T](\mathbf{x}_i-\delta\rho\mathbf{g})+\delta\rho\mathbf{g}\}=\mathbf{0}$$

to get the standard OGY control rule

$$\delta\rho=\frac{\lambda_u}{\lambda_u-1}\frac{\mathbf{f}_u\cdot\mathbf{x}}{\mathbf{f}_u\cdot\mathbf{g}}. \tag{2}$$

Notice that if the perturbation $\delta\rho$ shifts the target orbit along the unstable manifold, then $\mathbf{g}$ is parallel to $\mathbf{e}_u$, and any point in the unstable manifold and close enough to $\overline{\mathbf{x}}$ can be brought to the *target orbit itself* in one iteration of the control. By the same geometric reasoning, if the target orbit is shifted along the stable manifold as a result of the control perturbation, any system state lying initially in the stable manifold and close enough to $\overline{\mathbf{x}}$ can be brought to the target orbit in one iterate of the control procedure (see Fig. 1). In fact, for any $\mathbf{g}$ there exists a linear segment that maps directly to the target orbit. To see this, note that the condition that a control perturbation has placed the system state on the target orbit is $A(\mathbf{x}-\delta\rho\mathbf{g})+\delta\rho\mathbf{g}=0$. Therefore, the preimages of the target orbit are $\delta\rho(I-A^{-1})\mathbf{g}=\mathbf{x}$, a line of points along the vector $(I-A^{-1})\mathbf{g}$ parametrized by $\delta\rho$.

Recall that Eq. (2) gives the necessary perturbation $\delta\rho$ to place the system state in the stable manifold $\mathbf{e}_s$. Now suppose we want to ensure that $\mathbf{x}_{i+1}$ is also in the (linear) unstable manifold $\mathbf{e}_u$ after an application of the map, that is, we wish to ensure that the system state is mapped directly to the target orbit $\overline{\mathbf{x}}$. Then we must have

$$\mathbf{f}_s\cdot\{[\lambda_s\mathbf{e}_s\mathbf{f}_s^T+\lambda_u\mathbf{e}_u\mathbf{f}_u^T](\mathbf{x}_n-\delta\rho\mathbf{g})+\delta\rho\mathbf{g}\}=\mathbf{0}.$$

The necessary perturbation in this case is

$$\delta\rho=\frac{\lambda_s}{\lambda_s-1}\frac{\mathbf{f}_s\cdot\mathbf{x}}{\mathbf{f}_s\cdot\mathbf{g}}. \tag{3}$$

The requirement that $\mathbf{x}_{i+1}$ be in both the stable and unstable manifolds of the target orbit at time $n+1$ is

$$\delta\rho=\frac{\lambda_s}{\lambda_s-1}\frac{\mathbf{f}_s\cdot\mathbf{x}}{\mathbf{f}_s\cdot\mathbf{g}}=\frac{\lambda_u}{\lambda_u-1}\frac{\mathbf{f}_u\cdot\mathbf{x}}{\mathbf{f}_u\cdot\mathbf{g}},$$

$$\frac{\lambda_s(\lambda_u-1)}{\lambda_u(\lambda_s-1)}\frac{\mathbf{f}_u\cdot\mathbf{g}}{\mathbf{f}_s\cdot\mathbf{g}}\mathbf{f}_s\cdot\mathbf{x}=C\mathbf{f}_s\cdot\mathbf{x}=\mathbf{f}_u\cdot\mathbf{x}.$$

The set of initial conditions p at time n that map to the fixed point at time $i+1$ are such that if $\tilde{\mathbf{x}}_\rho$ is a vector collinear with p, the projections of $\tilde{\mathbf{x}}_i$ on the stable and unstable left eigenvectors are proportional, and therefore lie in a straight line. Thus, a linear segment of system states extending from $\overline{\mathbf{x}}$ to a point determined by the maximum allowable perturbation $\delta\rho_{max}$ can be mapped to the target orbit after one application of OGY control. This is the final step in the control procedure.

We can target $\tilde{\mathbf{x}}_\rho$ in the same way we targeted the stable manifold $\mathbf{e}_s$ for standard OGY control. Let $\mathbf{z}_\rho$ be such that $\mathbf{z}_\rho\cdot\tilde{\mathbf{x}}_\rho=0$. Then the condition

$$\mathbf{z}_\rho\cdot\{[\lambda_s\mathbf{e}_s\mathbf{f}_s^T+\lambda_u\mathbf{e}_u\mathbf{f}_u^T](\mathbf{x}_i-\delta\rho\mathbf{g})+\delta\rho\mathbf{g}\}=\mathbf{0}$$

ensures that the system state is in the set p, and leads to a control rule

$$\delta\rho=\frac{\lambda_s\mathbf{z}_\rho\cdot\mathbf{e}_s\mathbf{f}_s\cdot\mathbf{x}+\lambda_u\mathbf{z}_\rho\cdot\mathbf{e}_u\mathbf{f}_u\cdot\mathbf{x}}{\lambda_s\mathbf{z}_\rho\cdot\mathbf{e}_s\mathbf{f}_s\cdot\mathbf{g}+\lambda_u\mathbf{z}_\rho\cdot\mathbf{e}_u\mathbf{f}_u\cdot\mathbf{g}-\mathbf{z}_\rho\cdot\mathbf{g}}. \tag{4}$$

The control strategy for center manifold targeting (CMT) is to send the system state $\mathbf{x}_i$ to $\tilde{\mathbf{x}}_\rho$ with control rule (4) at iterate $i+1$, then to $\overline{\mathbf{x}}$ at time $i+2$ using control rule (2). Thus, for a two-dimensional linear map, we can place any initial condition in some control box about a target orbit directly into the target orbit after two iterates of the map using Eqs. (4) and (2) successively. For a nonlinear map or surface of section map of a continuous system, the method will be more or less effective depending on the linearity of the map in the controllable region. The controllable region, i.e., the preimages of all $\tilde{\mathbf{x}}_\rho$ is a parallelogram centered on the target orbit. To see this, note that the preimage of $\overline{\mathbf{x}}$ is

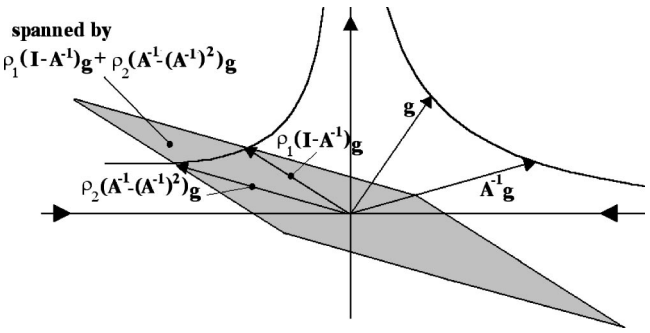

FIG. 2. The figure shows the perturbation vector **g** and its inverse images which span the first and second preimages of the target orbit.

$$\mathbf{x}_i(\rho)=\rho(\mathbf{g}-A^{-1}\mathbf{g}). \tag{5}$$

This is a vector of variable length parametrized by ρ (see Fig. 2).

For any particular point

$$\mathbf{x}_i(\delta_k\rho)=\delta_k\rho(\mathbf{g}-A^{-1}\mathbf{g}) \tag{6}$$

on $\mathbf{x}_i(\rho)$, we consider its preimages under perturbations parametrized by ρ. Since $\mathbf{x}_i(\delta_k\rho)-\rho\mathbf{g}=\delta_k\rho(\mathbf{g}-A^{-1}\mathbf{g})-\rho\mathbf{g}=A(\mathbf{x}_{i-1}-\rho\mathbf{g})$, we have

$$\mathbf{x}_{i-1}(\rho)=A^{-1}[\delta_k\rho(\mathbf{g}-A^{-1}\mathbf{g})-\rho\mathbf{g}]+\rho\mathbf{g}, \tag{7}$$

so the preimage of $\mathbf{x}_i(\rho)$ is

$$\mathbf{x}_{i-1}(\rho)=\delta_1\rho[A^{-1}-(A^{-1})^2]\mathbf{g}+\rho(I-A^{-1})\mathbf{g}. \tag{8}$$

Since A has a complete set of eigenvectors, $A^{-1}-(A^{-1})^2$ and $I-A^{-1}$ will differ, and Eq. (8) is the sum of a fixed vector parametrized by i and another parametrized by ρ. Let us replace $\delta_k\rho$ with ρ_2 and ρ by ρ_1, so that we have

$$\mathbf{x}_{i-1}(\rho)=\rho_2[A^{-1}-(A^{-1})^2]\mathbf{g}+\rho_1(I-A^{-1})\mathbf{g}. \tag{9}$$

This is a planar region parametrized by ρ_2 and ρ_1 (see Fig. 2).

Now ρ_2 is just a reparametrization of ρ_1, so the extent of the planar region is defined by the limits of ρ, the control parameter.

A similar calculation for the third preimage gives $\mathbf{x}_{i-2}(\rho_3,\rho_2,\rho_1)=\rho_3[(A^{-1})^2-(A^{-1})^3]\mathbf{g}+\rho_2[A^{-1}-(A^{-1})^2]\mathbf{g}+\rho_1(I-A^{-1})\mathbf{g}$. This is three vector that spans a slab centered on the target orbit.

In general, the mth preimage that will be an m-dimensional slab

$$\mathbf{x}(\rho_m,\rho_{m-1},\ldots,\rho_1)=\sum_{k=1}^{m}\rho_{m-k-1}[(A^{-1})^{k-1}-(A^{-1})^k]\mathbf{g},$$

where the ρ_j are all parameters linearly dependent on $\rho=\rho_1$, and indication of the iterate number of the variable has been dropped.

It is important to note here that the size of the controllable region depends on the direction of the perturbation vector **g** relative to the direction of the eigenvectors, for if **g** lies along an eigenvector that is used to increase the dimension of the slab, then the preimage of the $(m-1)$-dimensional ''subspace'' is that subspace itself, and there may be no route to the center manifold. Also, if the perturbation vector **g** lies in a subspace spanned by a set of eigenvectors all of whose eigenvalues are expanding, then there may be no route to the center manifold. So although CMT is capable of controlling systems with more than one unstable direction, it is essential that the perturbation vector not lie entirely in a subspace spanned by eigenvectors all of whose eigenvalues are expanding.

The significance of this construction is this: given a periodic orbit of any stability type, we can direct any orbit in the m slab into the $m-1$ slab in one iteration of the map via a perturbation of the control parameter $\rho=\rho_i$. The system therefore, can be controlled by a succession of parameter perturbations equal in number to the dimension of the system, ending in a completely controlled state. At each step the dimension of the controllable region is reduced by one, until the final step reduces it to a zero-dimensional region, the target orbit.

VI. CONTROL OF THE LOZI MAP BY CMT

As a concrete example, let us consider the Lozi [24] map. The Lozi map is a two-dimensional piecewise linear map whose dynamics are similar to those of the better known Hénon [25] map. The advantage of the Lozi map in this example is that we can compute every relevant parameter exactly, due to the linearity of the map, and the successful control can be demonstrated rigorously. We use a Lozi map of the form

$$x_{i+1}=(1+\rho)+ay_i-b|x_i|,$$

$$y_{i+1}=-x_i.$$

For $a=1/2$ and $b=7/4$ the Lozi map has a fixed point at $\bar{\mathbf{x}}=(4/13,-4/13)$, so near this point the dynamics are governed by

$$\mathbf{x}_{i+1}=\begin{bmatrix}-\frac{7}{4} & \frac{1}{2}\\ -1 & 0\end{bmatrix}\mathbf{x}_i.$$

The fixed point varies with ρ as $\{[4(1+\rho)/13],[-4(1+\rho)/13]\}$ so $(\partial/\partial\rho)\bar{\mathbf{x}}=\mathbf{g}=(4/13,-4/13)$ is the change in the fixed point with parameter ρ. For a particular perturbation $\delta\rho$ the change in fixed point is $\delta\rho\mathbf{g}=\delta\rho(4/13,-4/13)$. The eigenvalues and (right and left) eigenvectors of $\left[\begin{smallmatrix}-\frac{7}{4} & \frac{1}{2}\\ -1 & 0\end{smallmatrix}\right]$ are

$$\lambda_u=\frac{-7-\sqrt{17}}{8},\ \lambda_s=\frac{-7+\sqrt{17}}{8},$$

$$\mathbf{e}_u=\left(\frac{7+\sqrt{17}}{\sqrt{130+14\sqrt{17}}},4\sqrt{\frac{2}{65+7\sqrt{17}}}\right),$$

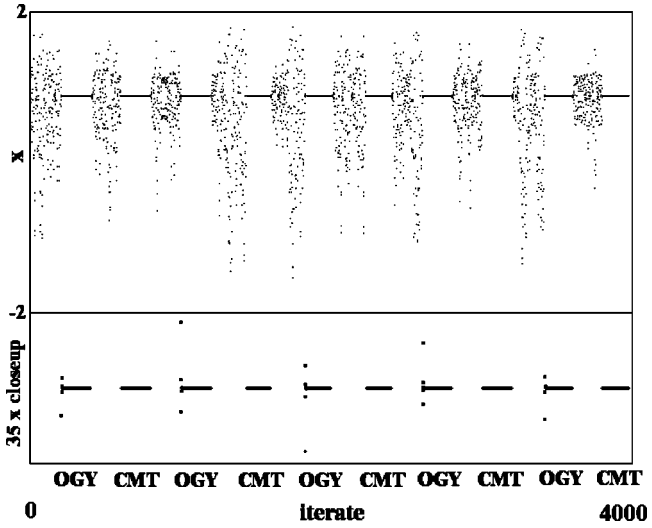

FIG. 3. This figure shows alternating control of the Lozi map by OGY and CMT, with the x coordinate on the vertical axis and time (in iterates) on the horizontal axis. Note the difference in the time to control. The lower graph shows a 35 times magnification of the controlled orbit. The first two iterates of each controlled orbit are not shown. The scale on the x axis just contains the attractor, and the units are nondimensional.

$$\mathbf{f}_u=\left(\sqrt{\frac{65+7\sqrt{17}}{34}},\frac{-7+\sqrt{17}}{8}\sqrt{\frac{65+7\sqrt{17}}{34}}\right),$$

$$\mathbf{e}_s=\left(\frac{7-\sqrt{17}}{\sqrt{130-14\sqrt{17}}},4\sqrt{\frac{2}{65-7\sqrt{17}}}\right),$$

$$\mathbf{f}_s=\left(-\sqrt{\frac{65-7\sqrt{17}}{34}},\frac{7+\sqrt{17}}{8}\sqrt{\frac{65-7\sqrt{17}}{34}}\right).$$

The equation for the Lozi map can be solved to find $\mathbf{z}_\rho=(1,0)$. For an arbitrary fixed point $\overline{\mathbf{s}}=(s,t)$ near $\overline{\mathbf{x}}$ and an arbitrary initial condition $\mathbf{x}_i=(q,r)$,

$$\mathbf{x}_{i+1}=\begin{bmatrix}-\frac{7}{4} & \frac{1}{2}\\ -1 & 0\end{bmatrix}(\mathbf{x}_i-\overline{\mathbf{s}}-\delta\rho\mathbf{g})+\overline{\mathbf{s}}+\delta\rho\mathbf{g}=(s,t+s-q).$$

Thus, when the formula for $\delta\rho$ is substituted in the above, the initial condition (q,r) is mapped to $(s,t+s-q)$, and the x_{i+1} coordinate is that of the fixed point, while the y_{i+1} coordinate varies about its nominal value of t, as expected. This line segment of initial conditions can then be mapped to the fixed point by the application of OGY control. Figure 3 shows a control session in which OGY and CMT control were applied alternately to a period one orbit of the Lozi map. The improvement in the control is striking. After one application of CMT, the orbit is in the preimage of the target orbit, and after the second application, the system state lies exactly in the target orbit, while OGY control takes many iterates to settle down.

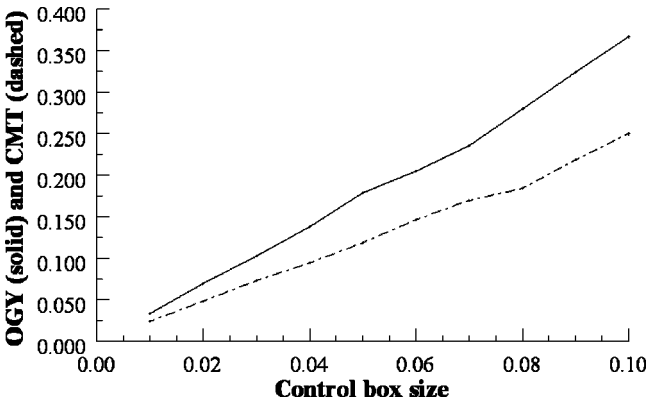

FIG. 4. This figure shows the average accumulated control perturbation over ten iterates for OGY and CMT control. The Hénon attractor for these parameters just fits in a box 3.5 by 3.5 nondimensional units, so the control box width ranges from $\approx 1/350$ to 1/35 the total attractor width.

VII. CONTROL OF THE HÉNON MAP BY CMT

The improvement of CMT over OGY is not as dramatic, when it is applied a nonlinear map like the Hénon map, as it is with the piecewise linear Lozi map, but it is still impressive. The Hénon map of the form

$$x_{i+1}=(a+\rho)-x_i^2+by,$$

$$y_{i+1}=x_i$$

is chaotic for $a=6/5, b=3/10$ with control parameter $\rho=0$, and at these values has a fixed point $\overline{\mathbf{x}}=(4/5,4/5)$. Near the fixed point, the Hénon map is governed approximately by the linear map

$$\mathbf{x}_{i+1}=A\mathbf{x}_i=\begin{bmatrix}-\frac{8}{5} & \frac{3}{10}\\ 1 & 0\end{bmatrix}\mathbf{x}_i.$$

We compared the OGY method to the CMT method by running 1000 trials on each of ten different control box sizes and plotting the average cumulative perturbation and deviation from the target orbit. For each trial a random initial condition inside the control box was given and both the OGY and CMT methods were allowed to stabilize it for ten iterations. Figure 4 shows the plot of the accumulated perturbation over ten iterates plotted against the size of the control box, and Fig. 5 shows the accumulated deviation from the target orbit. The CMT control offers approximately a 30% improvement in control cost over OGY, and about the same improvement in rate of convergence to the target orbit for this periodic orbit of the Hénon map.

VIII. HIGHER-DIMENSIONAL CONTROL BY CMT

The two-step procedure for a two-dimensional map can be extended to an n-step procedure for an n-dimensional map or surface of section map. Suppose a system $F(\mathbf{x},t,\rho)$ with surface of section map $f(\mathbf{x},i,\rho)$ is stabilized in a periodic orbit

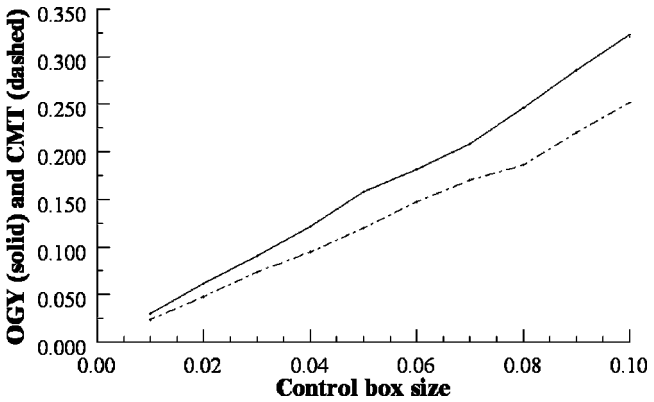

FIG. 5. The average accumulated deviation from the target orbit over ten iterates for OGY and CMT control. The Hénon attractor for these parameters just fits in a box 3.5 by 3.5 nondimensional units, so the control box width ranges from $\approx 1/350$ to 1/35 the total attractor width.

$\overline{\mathbf{x}}$ at time m. Then at time $m-1$ the system state was $\mathbf{x}_{m-1} = A_\rho^{-1}\mathbf{x}_m$. The set of states $\mathbf{x}_{m-1}$ parametrized by ρ lies in a straight line p because of the linearity of the map.

This line can be targeted by using a control rule derived from $\mathbf{z}_1 \cdot \mathbf{x}_m = \mathbf{z}_1 \cdot A(\mathbf{x}_{m-1} - \delta\rho\mathbf{g})$ where $\mathbf{z}_1$ is chosen orthogonal to the vector collinear with p, and A is now $n \times n$ and decomposed as

$$A = \begin{bmatrix} \mathbf{e}_1 & \cdots & \mathbf{e}_n \end{bmatrix} \begin{bmatrix} \lambda_1 & & \\ & \ddots & \\ & & \lambda_n \end{bmatrix} \begin{bmatrix} \mathbf{f}_1^T & \cdots & \mathbf{f}_n^T \end{bmatrix} \tag{10}$$

$$= [\lambda_1 \mathbf{e}_1 \mathbf{f}_1^T + \cdots + \lambda_n \mathbf{e}_n \mathbf{f}_n^T] \tag{11}$$

yielding the control rule

$$\delta\rho = \frac{\lambda_1 \mathbf{z}_1 \cdot \mathbf{e}_1 \mathbf{f}_1 \cdot \mathbf{x} + \cdots + \lambda_n \mathbf{z}_1 \cdot \mathbf{e}_n \mathbf{f}_n \cdot \mathbf{x}}{\lambda_1 \mathbf{z}_1 \cdot \mathbf{e}_1 \mathbf{f}_1 \cdot \mathbf{g} + \cdots + \lambda_n \mathbf{z}_1 \cdot \mathbf{e}_n \mathbf{f}_n \cdot \mathbf{g} - \mathbf{z}_1 \cdot \mathbf{g}}. \tag{12}$$

Similarly, the preimage of p under A^{-1} is generically a planar region p^2 centered on $\overline{\mathbf{x}}$ which can be targeted by requiring that $\mathbf{z}_2 \cdot (\mathbf{x}_{m-1} - \delta\rho\mathbf{g}) = \mathbf{z}_2 \cdot A(\mathbf{x}_{m-2} - \delta\rho\mathbf{g}) = \mathbf{0}$ where $\mathbf{z}_2$ is orthogonal to p^2. Likewise, the preimage of p^{n-1} under A^{-1} is an n-dimensional slab that can be targeted by the nth control rule

$$\delta\rho_n = \frac{\lambda_1 \mathbf{z}_n \cdot \mathbf{e}_1 \mathbf{f}_1 \cdot \mathbf{x} + \ \ldots \ + \lambda_n \mathbf{z}_n \cdot \mathbf{e}_n \mathbf{f}_n \cdot \mathbf{x}}{\lambda_1 \mathbf{z}_n \cdot \mathbf{e}_1 \mathbf{f}_1 \cdot \mathbf{g} + \ \ldots \ + \lambda_n \mathbf{z}_n \cdot \mathbf{e}_n \mathbf{f}_n \cdot \mathbf{g} - \mathbf{z}_n \cdot \mathbf{g}}. \tag{13}$$

IX. SUMMARY

In summary, I have proposed a control procedure that targets a succession of lower- and lower-dimensional slabs, each of which maps to the next lower-dimensional slab via a succession of control perturbations culminating in the mapping of a linear segment of system states directly to the target orbit by the standard OGY control rule. This procedure is not only applicable to the maps, but to the surface of section maps of continuous time systems. I have demonstrated the control procedure explicitly and in computer simulation on the piecewise linear Lozi map, and in a computer simulation of the Hénon map. The procedure is robust, and is superior to the OGY method in terms of time to achieve control. The CMT method is time optimal in that it achieves control in the least possible time for a linear map-based model.

[1] C. Grebogi, E. Ott, and J.A. Yorke, Phys. Rev. Lett. **64**, 1 (1990).
[2] F.J. Romeiras, C. Grebogi, E. Ott, and W.P. Dayawansa, Physica D **58**, 165 (1992).
[3] G. Chen, Int. J. Bifurcation Chaos Appl. Sci. Eng. **4**, 461 (1994).
[4] T. Shinbrot, E. Ott, C. Grebogi, and J.A. Yorke, Phys. Rev. Lett. **65**, 3215 (1990).
[5] E.M. Bollt and E.J. Kostelich, Phys. Lett. A **245**, 399 (1998).
[6] E. Bradley, in *Proceedings of the First Experimental Chaos Conference*, *Arlington*, *VA*, *1991*, edited by S. Vohra, M. Spano, M. Schlesinger, L. Pecora, and W. Ditto (World Scientific, Singapore, 1992), pp. 152–158.
[7] U. Dressler and G. Nitsche, Phys. Rev. Lett. **68**, 1 (1992).
[8] D. Auerbach, C. Grebogi, E. Ott, and J. Yorke, Phys. Rev. Lett. **69**, 3479 (1992).
[9] D.L. Hill, Int. J. Bifurcation Chaos Appl. Sci. Eng. **11**, 1753 (2001).
[10] K.A. Mirus and J.C. Sprott, Phys. Lett. A **254**, 275 (1999).
[11] I. Aranson, J. Levine, and L. Tsimring, Phys. Rev. Lett. **72**, 2561 (1994).
[12] M.E. Bleich and J.E.S. Socolar, Phys. Rev. E **54**, 17 (1996).
[13] P.M. Gade, Phys. Rev. E **57**, 7309 (1998).
[14] G. Hu, Z. Qu, and K. He, Int. J. Bifurcation Chaos Appl. Sci. Eng. **5**, 901 (1995).
[15] K. Pyragas, Phys. Lett. A **170**, 421 (1992).
[16] J.E.S. Socolar, D.W. Sukow, and D.J. Gauthier, Phys. Rev. E **50**, 3245 (1994).
[17] T.W. Carr and I.B. Schwartz, Physica D **96**, 17 (1996).
[18] B. Peng, V. Petrov, and K. Showalter, Physica A **188**, 210 (1992).
[19] E.R. Hunt, Phys. Rev. Lett. **67**, 1953 (1991).
[20] P. Parmananda, R.W. Rollins, and P. Sherard, Phys. Rev. E **47**, 1 (1993).
[21] C. Reyl, L. Flepp, R. Badii, and E. Brun, Phys. Rev. E **47**, 267 (1992).
[22] B. Epureanu and E. Dowell, Physica D **116**, 1 (1998).
[23] B. Epureanu and E. Dowell, Physica D **139**, 87 (2000).
[24] R. Lozi, J. Phys. (Paris), Colloq. **39**, 9 (1978).
[25] M. Henon, Commun. Math. Phys. **50**, 1 (1976).